Computational Investigation of the N(^{2}D)+ C_2H_4 and N(^{2}D)+ CH_2CHCN Reactions: Benchmark Analysis and Implications for Titan's Atmosphere

Luca Mancini[1(✉)], Emília Valença Ferreira de Aragão[1,2], and Marzio Rosi[3]

[1] Dipartimento di Chimica, Biologia e Biotecnologie, Università degli Studi di Perugia, 06123 Perugia, Italy
luca.mancini2@studenti.unipg.it
[2] Master-tec srl, Via Sicilia 41, 06128 Perugia, Italy
[3] Dipartimento di Ingegneria Civile ed Ambientale, Università degli Studi di Perugia, 06125 Perugia, Italy
marzio.rosi@unipg.it

Abstract. In the present contribution we report a theoretical investigation of the reactions of atomic nitrogen, in its first electronically excited ^{2}D state, with two different molecules: ethylene (C_2H_4) and acrylonitrile (CH_2CHCN), which appear to be important processes for the chemistry of Titan's atmosphere. The main reaction channels have been investigated through *ab initio* electronic structure calculations. Accurate quantum chemical calculations allowed the identification of the available pathways as a sequence of minimum and transition state structures, leading to the formation of different products, mainly related to H-displacement processes. Single point energy calculations have been performed at different levels of theory in order to establish a reasonable computational strategy for the analysis of astrochemically relevant gas phase neutral-neutral reactions.

Keywords: Computational chemistry · *Ab initio* calculations · Astrochemistry · Titan's atmosphere

1 Introduction

The appearence of life on Earth led to massive transformations of its geomorphology. As a result, studying planets and moons that are similar to the early Earth can be very helpful in providing a good picture of the early stages of our prebiotic chemistry. The best candidate for this purpose appears to be Titan, the largest moon of Saturn, that represents one of the only few moons of the Solar System which possess a thick atmosphere. Different space missions, including the

© The Author(s), under exclusive license to Springer Nature Switzerland AG 2023
O. Gervasi et al. (Eds.): ICCSA 2023 Workshops, LNCS 14105, pp. 705–717, 2023.
https://doi.org/10.1007/978-3-031-37108-0_45

last and famous Cassini-Huygens mission [1], provided new information about the composition and atmosphere of Saturn's moon. Titan's inner structure isn't completely known. Data coming from the latest missions can help to build a general model, according to which Titan's structure is characterized by five primary layers. The inner one is composed by a core of water-bearing silicate rock. The first core is surrounded by an ice-VI layer. This second layer is surrounded by a third layer of salty liquid water, covered by an outer crust of water ice. Finally, the surface is cover by a layer of organic molecules which grant to the moon the typical orange color. Despite several similarities of Titan's surface with the surface of our planet, the different temperature leads to different characteristic of Saturn's moon. In details the temperature reaches values down to 94 K on the surface of Titan (also resulting from 'greenhouse effects') and around 175 K in the stratosphere, while the overall surface pressure is 1.5 bar. As a consequence the surface is covered by water ice, which plays the role of Earth's rocks. The conditions of temperature and pressure appears to be closer to the ones typical of the triple point of methane, therefore, Titan's surface is crossed by rivers of flowing methane, which fills lakes and seas. The surface, in which few visible impact craters can be found, is covered by 'sand' composed of hydrocarbons, forming also dark dunes extending across Titan's equatorial region's landscape. Moreover, similarly to Earth, Titan shows several types of clouds formed by a plethora of different volatile species [2]. The main component of Titan's atmosphere has been revealed to be N_2 [3], followed by methane, and different other hydrocarbons (e.g. C_2H_6, C_2H_4, C_2H_2) [4]. In the recent years, different photochemical models have been developed [5–7], with the aim to include results from physical and chemical investigations to derive a representative simulations of Titan's atmosphere. Therefore, the analysis of chemical reactions involving molecular species containing nitrogen appears to be pivotal for the understanding of the chemistry of the atmosphere of Titan. From a chemical point of view, the N_2 molecule appears to have a high chemical stability. As a consequence, the main actor to drive the chemistry of Titan's atmosphere is "active nitrogen", namely atomic nitrogen in its ground and excited states $N(^4S)$ and $N(^2D)$, respectively. The main formation mechanisms for the two aforementioned species are related to the interaction of N_2 with EUV photons, as well as the impact of N_2 with energetic particles, including high energy free electrons. Unfortunately, the $N(^4S)$ ground state appears to be unreactive with closed-shell molecules, while $N(^2D)$ appears to be more reactive. This last species is metastable with a relatively long radiative lifetime [8] and an high energy content (it is 230 kJ mol^{-1} higher than the ground state) [9,10]. The reactivity of $N(^2D)$ with various partners has been the subject of several theoretical and experimental studies, with potential uses in the modeling of Titan's atmosphere (i.e. $N(^2D)+ C_2H_2$; C_2H_6; HC_3N) [11–13]. Together with the common and abundant C_2H_4 molecule, [14] another particularly relevant N-bearing molecule detected on Titan's atmosphere is acrylonitrile (CH_2CHCN). Interestingly, this last species is considered to be a promising candidate, considering also the possibility to form more complex and prebiotic species. After the initial data, obtained from the Cassini orbiter,

regarding the detection of the CH_2CHCNH^+ cation [15–18], the acrylonitrile molecule has been definitively detected using the ALMA interferometer [19,20]. One of the accepted formation routes of CH_2CHCN is the CN + C_2H_4 reaction [21–28], in which the dominant mechanism appears to be the elimination of atomic hydrogen, followed by the formation of CH_2CHCN. On the contrary, a lack of information is present regarding the possible destruction mechanisms of acrylonitrile. Following the directions of the aforementioned photochemical models, possible destruction routes of acrylonitrile are represented by the reactions with N(^{2}D) and CN radical. The two reactions analysed in the present contribution, N(^{2}D)+C_2H_4 and N(^{2}D)+CH_2CHCN, have already been investigated [29,30] combining an experimental investigation, performed through the crossed molecular beam (CMB) technique with mass spectrometric (MS) detection and time-of-flight (TOF) analysis, with accurate ab initio calculations in order to unveil the global reaction mechanism. In this work we present a theoretical investigation, performed at different levels of theory, of the main reaction pathways for the N(^{2}D)+C_2H_4 and N(^{2}D)+CH_2CHCN, which allows to derive a feasible computational strategy to be used for the study of different reaction between atomic nitrogen and hydrocarbons and/or nitrile molecules.

2 Theoretical Methods

The global doublet Potential Energy Surface (PES) for the two reactions, N(^{2}D) + C_2H_4 and N(^{2}D) + CH_2CHCN, has been analysed adopting a well-established computational strategy, already used for the investigation of several reactions [31–33]. In details, a first analysis has been performed through density functional calculations, with the B3LYP [34,35] functional, in conjunction with the correlation consistent valence polarized basis set aug-cc-pVTZ [36–38]. The same level of theory has been employed to calculate harmonic vibrational frequencies, in order to determine the nature of each stationary point, i.e. minimum if all the frequencies are real and saddle point if there is one, and only one, imaginary frequency. Subsequently, the energy of each stationary point has been computed with the more accurate coupled cluster theory including both single and double excitations and using a perturbative estimate of the effect of the triple excitations (the CCSD(T) level) [39–41], with the same basis set aug-cc-pVTZ. The zero-point correction (computed using the scaled harmonic vibrational frequencies obtained at the B3LYP/aug-cc-pVTZ level) has been added in order to correct the energies at 0 K. Additionally, more accurate calculations for the stationary points involved in the main reaction channels have been performed at the CCSD(T) level corrected with a Density Fitted (DF) MP2 extrapolation to the complete basis set (CBS) and with corrections for core electrons excitations. In particular, the energies have been computed as:

$$E = E(CCSD(T)/aug-cc-pVTZ) + [E(CCSD(T,core)/cc-pVTZ) - E(CCSD(T)/cc-pVTZ)] + [E(DF-MP2/CBS) - E(DF-MP2/aug-cc-pVTZ)]$$

where E(DF-MP2/CBS) is defined as:

$$E(DF-MP2/CBS) = E[(DF-MP2)/aug-cc-pVQZ)] + 0.5772 * [E(DF-MP2/aug-cc-pVQZ) - E(DF-MP2/aug-cc-pVTZ)]$$

The E(DF-MP2/CBS) extrapolation has been performed using Martin's two parameter scheme [42], by performing a series of ab initio calculations using the MP2 method and different basis set (including aug-cc-pVTZ and aug-cc-pVQZ).

The experimental separation [43] N(^{4}S)-N(^{2}D) of 230.0 kJ mol^{-1} has been added to the energy of N(^{4}S) at all the levels of calculations in order to have a more accurate estimation of the energy of N(^{2}D). All calculations have been carried out using GAUSSIAN 09 [44] and Molpro [45] while the analysis of the vibrational frequencies has been done using MOLDEN [46,47].

3 Results

3.1 The N(^{2}D)+C_2H_4 Reaction

The potential energy surface obtained for the N(^{2}D)+C_2H_4 reaction is reported in Fig. 1. As already explained, the energy of the stationary points has been evaluated at different levels of theory (B3LYP/aug-cc-pVTZ, CCSD(T)/aug-cc-pVTZ, CCSD(T)/CBS). The results obtained from the different investigations are reported in Table 1. For the sake of simplicity, in the following description only the more accurate results (i.e. the CCSD(T)/CBS energy values) are described. As is evident, the interaction of atomic nitrogen with the ethylene system, which results in the attack of N(^{2}D) on the C-C double bond of C_2H_4, and the subsequent formation of the MIN1 intermediate (located 447 kJ mol^{-1} below the reactant energy asymptote), represents the first step of the reaction. When MIN1 is created, it can immediately go through an H-displacement process, which creates the cyclic CH_2(N)CH radical. The process has a total exothermicity of 264 kJ mol^{-1}, while the product channel has a barrier of 195 kJ mol^{-1}. With a bond distance of 2.075 Å, the associated transition state, TS2, exhibits the dissolution of a C-H bond. For the aforementioned MIN1, an alternative outcome is represented by the isomerization to MIN2, through the breaking of the C-C σ-bond. The process is characterized by a barrier (represented by TS1) of 114 kJ mol^{-1}. Once formed, MIN2, located 517 kJ mol^{-1} below the energy of the reactants, can result in the atomic hydrogen and the CH_2NCH linear radical being formed. This reaction channel is located 226 kJ mol^{-1} under the energy of the N(^{2}D)+C_2H_4 reagents. A transition state, TS3, located 226 kJ mol^{-1} below the energy of the reactants, was identified for the H-displacement process. This last process is characteirzed by a barrier almost equal to the endothermicity of

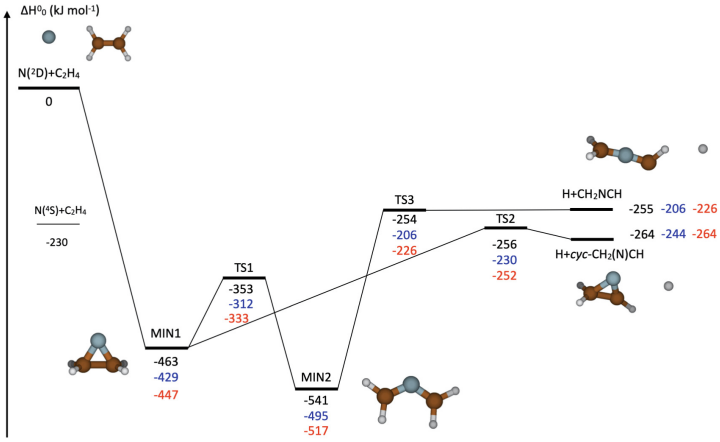

Fig. 1. Schematic representation of the potential energy surface for the N(^{2}D) $+C_2H_4$ reaction with energies evaluated at the B3LYP/aug-cc-pVTZ (in black), CCSD(T)/aug-cc-pVTZ (in blue) and CCSD(T)/CBS (in red) level of theory. (Color figure online)

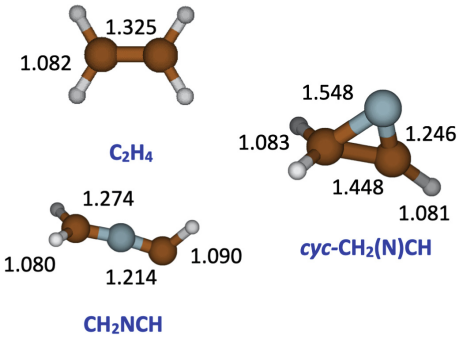

Fig. 2. Bond distances (in Å) for the reactant (C_2H_4) and products of the N(^{2}D) $+C_2H_4$ reaction.

the reaction at all the levels of theory. Therefore, the barrier is not very relevant and can be neglected in the global PES. Figures 2 and 3 show the geometry (bond distances in Å) of all the stationary points, including the C_2H_4 reactant and the two products, evaluated through the previous described DFT calculations.

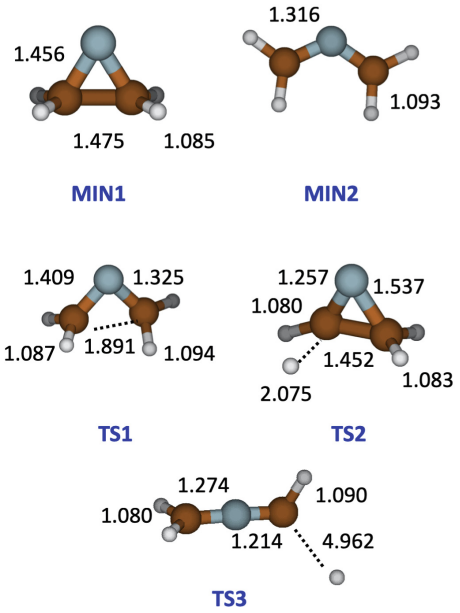

Fig. 3. Bond distances (in Å) for the minima and transition states of the N(^{2}D) +C_2H_4 reaction.

Table 1. Enthalpy changes (ΔH_0^0) and barrier height, in kJ mol^{-1}, for the main channels of the N(^{2}D) +C_2H_4 reaction evualated at the B3LYP/aug-cc-pVTZ, CCSD(T)/aug-cc-pVTZ and CCSD(T)/CBS level, respectively.

Reaction Channel	B3LYP/aug-cc-pVTZ		CCSD(T)/aug-cc-pVTZ		CCSD(T)/CBS	
	ΔH_0^0	*Barrier*	ΔH_0^0	*Barrier*	ΔH_0^0	*Barrier*
$N(^2D) + C_2H_4 \rightarrow MIN1$	–463	–	–429	–	–447	–
$MIN1 \rightarrow H + cyc - CH_2(N)CH$	199	207	185	199	183	195
$MIN1 \rightarrow MIN2$	–78	110	–66	117	–70	114
$MIN2 \rightarrow H + CH_2NCH$	286	287	289	289	291	291

3.2 The N(^{2}D)+ CH_2CHCN Reaction

The potential energy surface obtained for the N(^{2}D)+CH_2CHCN reaction, reported in Fig. 4, shows some similarities with the one obtained for the previous reported reaction. The main difference is due to the presence of a CN group in the place of an hydrogen atom, which removes the symmetry of the molecule. As a consequence, the PES appears to be more complex and characterized by an increased number of possible reaction pathways.

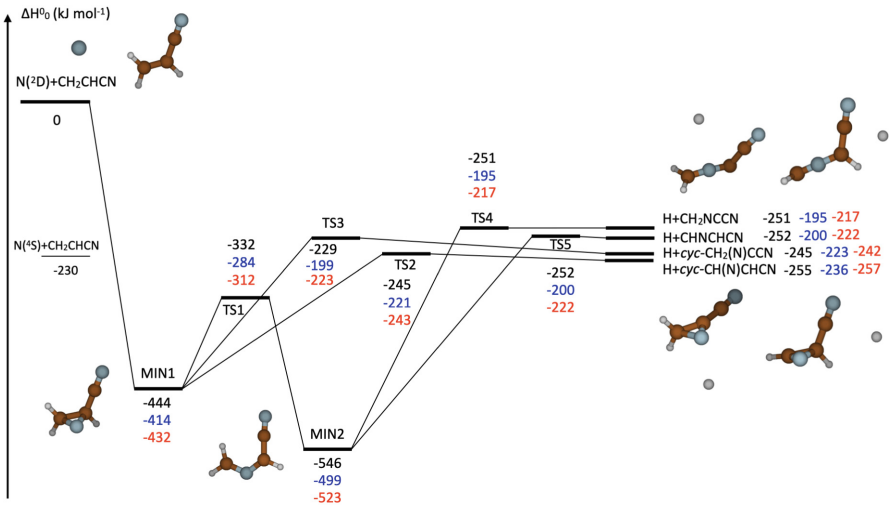

Fig. 4. Schematic representation of the potential energy surface for the N(^{2}D) +CH_2CHCN reaction with energies evaluated at the B3LYP/aug-cc-pVTZ (in black), CCSD(T)/aug-cc-pVTZ (in blue) and CCSD(T)/CBS (in red) level of theory. (Color figure online)

Also in this case, among all the calculated values of energy, only the more accurate results (i.e. the CCSD(T)/CBS energy values) are described. The values of enthalpy changes and barrier heights evaluated at the different level of theory are reported in Table 2. Similarly to case of the N(^{2}D)+C_2H_4 reaction, the first step is represented by the attack of N(^{2}D) to the C-C double bond of CH_2CHCN, with the formation of the MIN1 intermediate, located 432 kJ mol^{-1} below the reactant energy asymptote and characterized by a cyclic C(N)C structure. Once formed, MIN1 can undergo two different H-displacement process, depending on which H atom is eliminated, leading to the formation of two cyclic isomers CH_2(N)CCN and CH(N)CHCN. The global exothermicity of the two products is 242 kJ mol^{-1} and 257 kJ mol^{-1}, respectively. Two different transition states have been identified for the related H-displacement process, TS2 and TS3, representing a barrier of 189 kJ mol^{-1} and 209 kJ mol^{-1} respectively. The breaking of the C-C bond in MIN1, represented by the TS1 transition state (which shows an energy of 312 kJ mol^{-1} below the reactant energy asymptote), leads to the formation of the linear intermediate MIN2, whose global exothermicity is 523 kJ mol^{-1}. Once formed, MIN2 can lead to the formation of atomic hydrogen, together with the two CH_2NCCN and CHNCHCN linear radicals, located 217 kJ mol^{-1} and 222 kJ mol^{-1} under the energy of the N(^{2}D)+CH_2CHCN reactants. Two possible transition states, TS4 and TS5, have been identified in the PES. Similarly to the case of the previous described reaction, the energy of the two saddle points is almost equal to the endothermicity of the reaction channel at all the levels of theory. Therefore, the barriers are not very relevant and can be

neglected in the global PES. Figures 5 and 6 show the geometry (bond distances in A) of all the stationary points, including the CH_2CHCN reactant and the four products, evaluated through the previous described DFT calculations.

Table 2. Enthalpy changes (ΔH_0^0) and barrier height, in kJ mol^{-1}, for the main channels of the N(^{2}D) +CH_2CHCN reaction evualated at the B3LYP/aug-cc-pVTZ, CCSD(T)/aug-cc-pVTZ and CCSD(T)/CBS level, respectively.

Reaction Channel	B3LYP/aug-cc-pVTZ		CCSD(T)/aug-cc-pVTZ		CCSD(T)/CBS	
	ΔH_0^0	*Barrier*	ΔH_0^0	*Barrier*	ΔH_0^0	*Barrier*
$N(^2D) + CH_2CHCN \rightarrow MIN1$	–444	–	–414	–	–432	–
$MIN1 \rightarrow H + cyc - CH_2(N)CCN$	199	215	191	215	190	209
$MIN1 \rightarrow H + cyc - CH(N)CHCN$	189	199	178	193	175	189
$MIN1 \rightarrow MIN2$	–55	112	–85	130	–91	120
$MIN2 \rightarrow H + CH_2NCCN$	248	248	304	304	306	306
$MIN2 \rightarrow H + CHNCHCN$	247	247	299	299	301	301

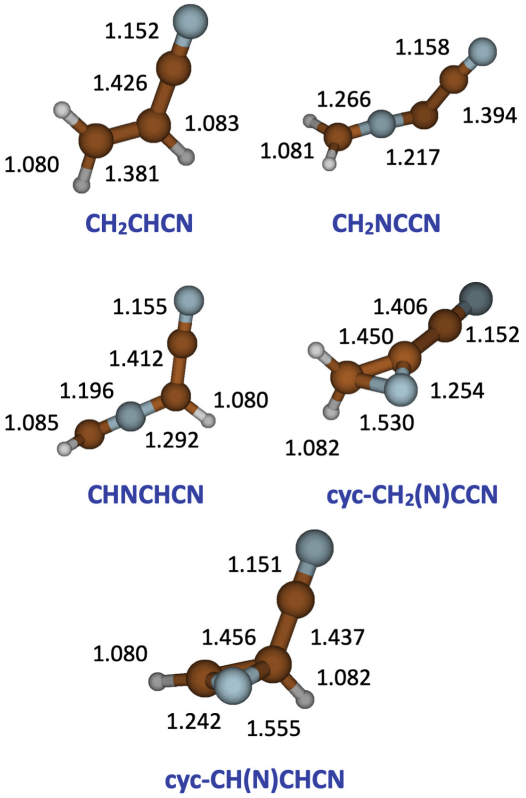

Fig. 5. Bond distances (in Å) for the reactant (CH_2CHCN) and products of the N(^{2}D) + CH_2CHCN reaction.

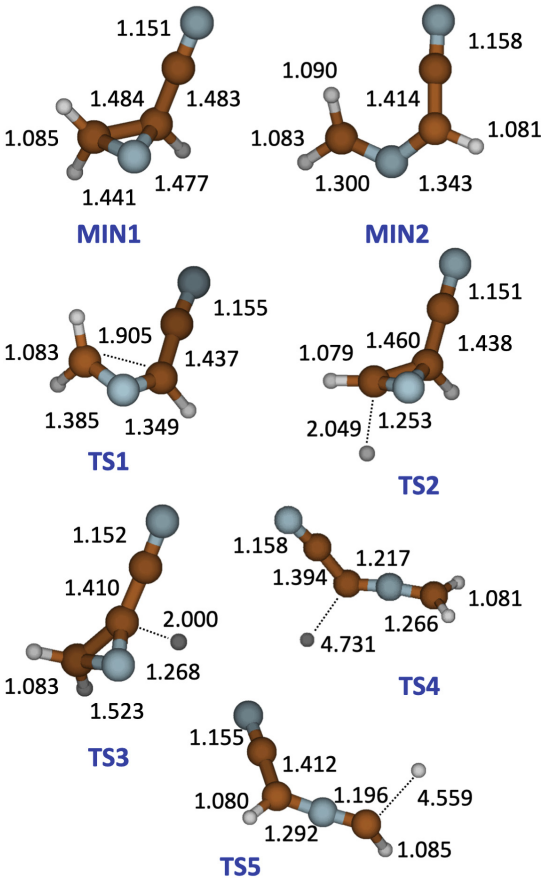

Fig. 6. Bond distances (in Å) for the minima and transition states of the N(^{2}D) + CH_2CHCN reaction.

4 Discussion

The two reactions N(^{2}D)+C_2H_4 and N(^{2}D) +CH_2CHCN show some similarities, especially considering the initial bimolecular approach. The main differences can be ascribed to the presence of the CN group. Indeed, the acrilonitrile molecule (CH_2CHCN) can be considered as ethylene (C_2H_4) with a CN group in place of an H atom. The presence of this cyano moiety removes the symmetry of the molecule, leading to a more complex reaction scheme, characterized by a double number of possible reaction paths and product channels. The high electrophilicity of the nitrogen, drawn to the double bond's electron density in both processes, is what propels N(^{2}D)'s attack on the companion molecule. Due to the presence of two C-N bonds involving the two ethylenic carbon atoms in a cyclic structure, the two reactions result in the development of a cyclic intermediate. In the case of the N(^{2}D)+C_2H_4 reaction, the formation of a cyclic species is possible, thanks

to a H-displacement process directly after the initial attack. In the case of the reaction with acrylonitrile, instead, two main cyclic products can be formed. Alternatively, the C(N)C ring opening process has been identified as the cause of the generation of linear intermediates, which can immediately undergo an H-displacement process, depending on the hydrogen atom which is eliminated from the different carbon atoms. In the present work, after a first identification of the main reaction paths in the PES, the energy of the various stationary points have been calculated at different levels of theory. As can be seen from the data reported in Table 1 and Table 2, some differences can be noticed in the values of energy. In particular, DFT calculations tend to overestimate the energy, while the more accurate CCSD(T)/CBS level provides more reliable data. Considering the difference between the obtained data, the use of coupled-cluster theory, in conjunction with the aug-cc-pVTZ basis set leads to accurate data in a less time consuming approach.

5 Conclusions

In the present contribution we report a theoretical investigation of the potential energy surface for the two $N(^2D)+C_2H_4$ and $N(^2D)$ $+CH_2CHCN$ reactions, that are important for the chemistry of planetary atmospheres, in particular in the atmosphere of Titan. Both the processes have been found to be barrierless. This is a key component for astrochemical reactions, along with the existence of stationary points below the reactant energy asymptote. In actuality, Titan's low temperatures indicate a hostile chemical environment where only exothermic and barrierless reactions may occur. Following this formalization, it appears that the two $N(2D)+C_2H_4$ and $N(2D)$ $+CH_2CHCN$ reactions are viable and significant paths to add knowledge about the chemistry of nitrogen-bearing molecules on Titan's atmosphere. A complete analysis of the overall PES, together with a kinetic investigation of the rate constants and branching ratios, will allow to understand the importance of the title processes and to improve the chemical models of the atmosphere of Titan. Additionally, a combined approach using DFT methods for geometry optimizations, followed by a CCSD(T) analysis of the energy, appears to be the best compromise between chemical accuracy and computational cost for the analysis of reactions involving $N(^2D)$ and hydrocarbons in Titan's atmosphere.

Aknowledgements. This project has received funding from the Italian MUR (PRIN 2020, "Astrochemistry beyond the second period elements", Prot. 2020AFB3FX) and from the European Union's Horizon 2020 research and innovation programme under the Marie Skłodowska-Curie grant agreement No 811312 for the project 'Astro-Chemical Origins' (ACO). The authors thank the Herla Project - Università degli Studi di Perugia (http://www.hpc.unipg.it/hosting/vherla/vherla.html) for allocated computing time. The authors thank the Dipartimento di Ingegneria Civile ed Ambientale of the University of Perugia for allocated computing time within the project "Dipartimenti di Eccellenza 2018-2022".

References

1. Brown, R.H., Lebreton, J.P., Waite, J.H.: Titan from cassini-huygens (2009)
2. Hörst, S.M.: Titan's atmosphere and climate. J. Geophys. Res. Planets **122**(3), 432–482 (2017)
3. Lindal, G.F., Wood, G., Hotz, H., Sweetnam, D., Eshleman, V., Tyler, G.: The atmosphere of titan: an analysis of the voyager 1 radio occultation measurements. Icarus **53**(2), 348–363 (1983)
4. Hanel, R., et al.: Infrared observations of the saturnian system from voyager 1. Science **212**(4491), 192–200 (1981)
5. Yung, Y.L., Allen, M., Pinto, J.P.: Photochemistry of the atmosphere of titan: comparison between model and observations. Astrophys. J. Suppl. Ser. **55**(3), 465–506 (1984)
6. Lavvas, P., Coustenis, A., Vardavas, I.: Coupling photochemistry with haze formation in titan's atmosphere, part ii: results and validation with Cassini/Huygens data. Planet. Space Sci. **56**(1), 67–99 (2008)
7. Vuitton, V., Yelle, R., Klippenstein, S., Hörst, S., Lavvas, P.: Simulating the density of organic species in the atmosphere of titan with a coupled ion-neutral photochemical model. Icarus **324**, 120–197 (2019)
8. Dutuit, O., et al.: Critical review of n, n^+, n_2^+, n^{++}, and n_2^{++} main production processes and reactions of relevance to titan's atmosphere. Astrophys. J. Suppl. Ser. **204**(2), 20 (2013)
9. Herron, J.T.: Evaluated chemical kinetics data for reactions of n(^{2}d), n_2)), and n_2(* 3* u+) in the gas phase (1999)
10. Schofield, K.: Critically evaluated rate constants for gaseous reactions of several electronically excited species. J. Phys. Chem. Ref. Data **8**(3), 723–798 (1979)
11. Balucani, N., et al.: Cyanomethylene formation from the reaction of excited nitrogen atoms with acetylene: a crossed beam and ab initio study. J. Am. Chem. Soc. **122**(18), 4443–4450 (2000)
12. Balucani, N., et al.: Formation of nitriles and imines in the atmosphere of titan: combined crossed-beam and theoretical studies on the reaction dynamics of excited nitrogen atoms n(^{2}d) with ethane. Faraday Discuss. **147**, 189–216 (2010)
13. Liang, P., et al.: Combined crossed molecular beams and computational study on the n(^{2}d)+ HCCCN (x^1 σ+) reaction and implications for extra-terrestrial environments. Mol. Phys. **120**(1–2), e1948126 (2022)
14. Vinatier, S., et al.: Analysis of Cassini/CIRS limb spectra of titan acquired during the nominal mission: I. hydrocarbons, nitriles and co_2 vertical mixing ratio profiles. Icarus **205**(2), 559–570 (2010)
15. Cui, J., et al.: Analysis of titan's neutral upper atmosphere from Cassini ion neutral mass spectrometer measurements. Icarus **200**(2), 581–615 (2009)
16. Vuitton, V., Yelle, R., McEwan, M.: Ion chemistry and n-containing molecules in titan's upper atmosphere. Icarus **191**(2), 722–742 (2007)
17. Magee, B.A., Waite, J.H., Mandt, K.E., Westlake, J., Bell, J., Gell, D.A.: INMS-derived composition of titan's upper atmosphere: analysis methods and model comparison. Planet. Space Sci. **57**(14–15), 1895–1916 (2009)
18. Müller-Wodarg, I., Griffith, C.A., Lellouch, E., Cravens, T.E.: Titan: Interior, Surface, Atmosphere, and Space Environment, vol. 14. Cambridge University Press, Cambridge (2014)
19. Palmer, M.Y., et al.: ALMA detection and astrobiological potential of vinyl cyanide on titan. Sci. Adv. **3**(7), e1700022 (2017)

20. Lai, J.Y., et al.: Mapping vinyl cyanide and other nitriles in titan's atmosphere using alma. Astron. J. **154**(5), 206 (2017)
21. Sims, I.R., et al.: Rate constants for the reactions of CN with hydrocarbons at low and ultra-low temperatures. Chem. Phys. Lett. **211**(4–5), 461–468 (1993)
22. Balucani, N., et al.: Crossed beam reaction of cyano radicals with hydrocarbon molecules. iii. chemical dynamics of vinylcyanide (c_2h_3 CN; x^1a') formation from reaction of CN ($x^2\sigma^+$) with ethylene, c_2h_4 (x^1a_g). J. Chem. Phys. **113**(19), 8643–8655 (2000)
23. Balucani, N., et al.: Formation of nitriles in the interstellar medium via reactions of cyano radicals, CN (x $2\sigma+$), with unsaturated hydrocarbons. Astrophys. J. **545**(2), 892 (2000)
24. Balucani, N., Asvany, O., Osamura, Y., Huang, L., Lee, Y., Kaiser, R.: Laboratory investigation on the formation of unsaturated nitriles in titan's atmosphere. Planet. Space Sci. **48**(5), 447–462 (2000)
25. Leonori, F., Petrucci, R., Wang, X., Casavecchia, P., Balucani, N.: A crossed beam study of the reaction CN+C_2H_4 at a high collision energy: the opening of a new reaction channel. Chem. Phys. Lett. **553**, 1–5 (2012)
26. Balucani, N., et al.: A combined crossed molecular beams and theoretical study of the reaction CN+C_2H_4. Chem. Phys. **449**, 34–42 (2015)
27. Vereecken, L., De Groof, P., Peeters, J.: Temperature and pressure dependent product distribution of the addition of CN radicals to C_2H_4. Phys. Chem. Chem. Phys. **5**(22), 5070–5076 (2003)
28. Gannon, K.L., Glowacki, D.R., Blitz, M.A., Hughes, K.J., Pilling, M.J., Seakins, P.W.: H atom yields from the reactions of CN radicals with c_2h_2, c_2h_4, c_3h_6, trans-2-c_4h_8, and iso-c_4h_8. J. Phys. Chem. A **111**(29), 6679–6692 (2007)
29. Balucani, N., et al.: Combined crossed beam and theoretical studies of the n(^{2}d)+ c_2h_4 reaction and implications for atmospheric models of titan. J. Phys. Chem. A **116**(43), 10467–10479 (2012)
30. Vanuzzo, G., et al.: The n(^{2}d)+ ch_2chcn (vinyl cyanide) reaction: a combined crossed molecular beam and theoretical study and implications for the atmosphere of titan. J. Phys. Chem. A **126**(36), 6110–6123 (2022)
31. Marchione, D., et al.: Unsaturated dinitriles formation routes in extraterrestrial environments: a combined experimental and theoretical investigation of the reaction between cyano radicals and cyanoethene (c_2h_3cn). J. Phys. Chem. A **126**(22), 3569–3582 (2022)
32. Rosi, M., et al.: Possible scenarios for sis formation in the interstellar medium: electronic structure calculations of the potential energy surfaces for the reactions of the SiH radical with atomic sulphur and S_2. Chem. Phys. Lett. **695**, 87–93 (2018)
33. Mancini, L., Trinari, M., de Aragão, E.V.F., Rosi, M., Balucani, N.: The s^+(^{4}s)+ sih_2 ($^1a_1$) reaction: toward the synthesis of interstellar SiS. In: Gervasi, O., Murgante, B., Misra, S., Rocha, A.M.A.C., Garau, C. (eds.) Computational Science and Its Applications – ICCSA 2022 Workshops. ICCSA 2022. LNCS, vol. 13378, pp. 233–245. Springer, Cham (2022). https://doi.org/10.1007/978-3-031-10562-3_17
34. Becke, A.D.: A new mixing of Hartree-Fock and local density-functional theories. J. Chem. Phys. **98**(2), 1372–1377 (1993)
35. Stephens, P.J., Devlin, F.J., Chabalowski, C.F., Frisch, M.J.: Ab initio calculation of vibrational absorption and circular dichroism spectra using density functional force fields. J. Phys. Chem. **98**(45), 11623–11627 (1994)

36. Dunning Jr, T.H.: Gaussian basis sets for use in correlated molecular calculations. I. The atoms boron through neon and hydrogen. J. Chem. Phys. **90**(2), 1007–1023 (1989)
37. Woon, D.E., Dunning Jr, T.H.: Gaussian basis sets for use in correlated molecular calculations. III. The atoms aluminum through argon. J. Chem. Phys. **98**(2), 1358–1371 (1993)
38. Kendall, R.A., Dunning Jr, T.H., Harrison, R.J.: Electron affinities of the first-row atoms revisited. Systematic basis sets and wave functions. J. Chem. Phys. **96**(9), 6796–6806 (1992)
39. Bartlett, R.J.: Many-body perturbation theory and coupled cluster theory for electron correlation in molecules. Annu. Rev. Phys. Chem. **32**(1), 359–401 (1981)
40. Raghavachari, K., Trucks, G.W., Pople, J.A., Head-Gordon, M.: A fifth-order perturbation comparison of electron correlation theories. Chem. Phys. Lett. **157**(6), 479–483 (1989)
41. Olsen, J., Jo/rgensen, P., Koch, H., Balkova, A., Bartlett, R.J.: Full configuration-interaction and state of the art correlation calculations on water in a valence double-zeta basis with polarization functions. J. Chem. Phys. **104**(20), 8007–8015 (1996)
42. Martin, J.M.: Ab initio total atomization energies of small molecules-towards the basis set limit. Chem. Phys. Lett. **259**(5–6), 669–678 (1996)
43. Moore, C.E.: Atomic Energy Levels. US Department of Commerce, National Bureau of Standards (1949)
44. Frisch, M., et al.: Gaussian 09, rev. A. 02, Gaussian. Inc., Wallingford, CT (2009)
45. Werner, H.J., et al.: The molpro quantum chemistry package. J. Chem. Phys. **152**(14), 144107 (2020)
46. Schaftenaar, G., Noordik, J.H.: Molden: a pre-and post-processing program for molecular and electronic structures. J. Comput. Aided Mol. Des. **14**(2), 123–134 (2000)
47. Schaftenaar, G., Vlieg, E., Vriend, G.: Molden 2.0: quantum chemistry meets proteins. J. Comput. Aided Mol. Des. **31**(9), 789–800 (2017). https://doi.org/10.1007/s10822-017-0042-5